7 Charm-hadron decay constants and form factors

Authors: Y. Aoki, M. Della Morte, E. Lunghi, S. Meinel, C. Monahan, A. Vaquero

Leptonic and semileptonic decays of charmed D and D_s mesons or Λ_c and other charm baryons occur via charged W-boson exchange, and are sensitive probes of $c \to d$ and $c \to s$ quark flavour-changing transitions. Given experimental measurements of the branching fractions combined with sufficiently precise theoretical calculations of the hadronic matrix elements, they enable the determination of the CKM matrix elements $|V_{cd}|$ and $|V_{cs}|$ (within the Standard Model) and a precise test of the unitarity of the second row of the CKM matrix. Here, we summarize the status of lattice-QCD calculations of the charmed leptonic decay constants. Significant progress has been made in charm physics on the lattice in recent years, largely due to the availability of gauge configurations produced using highly-improved lattice-fermion actions that enable treating the c quark with the same action as for the u, d, and s quarks.

This section updates the corresponding section in the last review (FLAG 21 [1]) for results that appeared before April 30, 2024. As in FLAG 19 [2] and FLAG 21 [1], we limit our review to results based on modern simulations with reasonably light pion masses (below approximately 500 MeV). This excludes results with two flavours in the sea, even if they use light pion masses. $N_f = 2$ results can still be checked in previous FLAG editions.

For the heavy-meson decay constants and mixing parameters, estimates of the quantity $\delta(a_{\min})$ described in Sec. 2.1.2 are provided for all computations entering the final FLAG averages or ranges. For heavy-hadron semileptonic-decay form factors, implementing this data-driven continuum-limit criterion was found to be not feasible. The problem is that these quantities are functions of the momentum transfer in addition to the other lattice parameters, and many calculations are based on global fits whose reconstruction was not possible.

Following our review of lattice-QCD calculations of $D_{(s)}$-meson leptonic decay constants and charm-hadron semileptonic form factors, we then interpret our results within the context of the Standard Model. We combine our best-determined values of the hadronic matrix elements with the most recent experimentally-measured branching fractions to obtain $|V_{cd(s)}|$ and test the unitarity of the second row of the CKM matrix.

7.1 Leptonic decay constants f_D and f_{D_s}

In the Standard Model, and up to electromagnetic corrections, the decay constant $f_{D_{(s)}}$ of a pseudoscalar D or D_s meson is related to the branching ratio for leptonic decays mediated by a W boson through the formula

$$\mathcal{B}(D_{(s)} \to \ell\nu_\ell) = \frac{G_F^2 |V_{cq}|^2 \tau_{D_{(s)}}}{8\pi} f_{D_{(s)}}^2 m_\ell^2 m_{D_{(s)}} \left(1 - \frac{m_\ell^2}{m_{D_{(s)}}^2}\right)^2 , \tag{124}$$

where q is d or s and V_{cd} (V_{cs}) is the appropriate CKM matrix element for a D (D_s) meson. The branching fractions have been experimentally measured by CLEO, Belle, Babar and BES with a precision around 2.5–4.5% for both the D and the D_s-meson decay modes [3]. When combined with lattice results for the decay constants, they allow for determinations of $|V_{cs}|$ and $|V_{cd}|$.

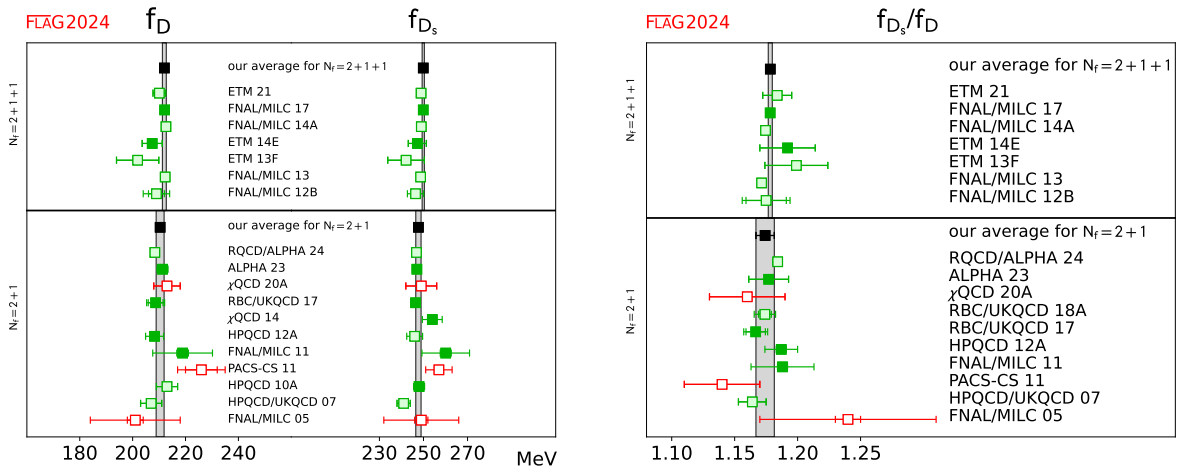

Figure 16: Decay constants of the D and D_s mesons [values in Tab. 28 and Eqs. (126-131)]. As usual, full green squares are used in the averaging procedure, pale green squares have either been superseded by later determinations or are only published in Proceedings or have not been published within the current deadline (April 30, 2024), while pale red squares do not satisfy the criteria. The black squares and grey bands indicate our averages.

The decay constants $f_{D_{(s)}}$ are defined through the matrix elements of the axial current

$$\langle 0|A^{\mu}_{cq}|D_q(p)\rangle = i f_{D_q}\, p^{\mu}_{D_q}\,, \tag{125}$$

with $q = d, s$ and $A^{\mu}_{cq} = \bar{c}\gamma^{\mu}\gamma_5 q$. Such matrix elements can be extracted from Euclidean two-point functions computed on the lattice.

Results for $N_f = 2+1$ and $2+1+1$ dynamical flavours are summarized in Tab. 28 and Fig. 16. Since the publication of FLAG 21, a handful of results for f_D and f_{D_s} have appeared, as described below. We consider isospin-averaged quantities, although, in a few cases, results for f_{D^+} are quoted (see, for example, the FNAL/MILC 11,14A and 17 computations, where the strong-isospin-breaking effect given by the difference between f_D and f_{D^+} has been estimated to be around 0.5 MeV).

For the first time, we restrict the review here to results obtained using $N_f = 2+1$ and $2+1+1$ dynamical flavours. No new results with $N_f = 2$ appeared since 2019 and they have been presented in previous FLAG reviews.

Another novelty is the re-inclusion of the quantity $\delta(a_{\min})$ described in the Introduction. Our working group introduced and applied this quantity in FLAG 13 [4], but it was not applied in following reviews. As computations have become increasingly precise and often dominated by systematic uncertainties, we believe that a closer scrutiny of the continuum extrapolations is needed since such extrapolations usually produce one of the largest systematic errors. Here, we provide (where possible) an estimate of $\delta(a_{\min})$ for all computations entering the final FLAG averages or ranges. Those estimates do not need to be very precise as the natural size of the error on $\delta(a_{\min})$ is $\mathcal{O}(1)$.

Two new results appeared with $N_f = 2+1$. In Ref. [13] (ALPHA 23) maximally twisted Wilson valence fermions (for light and heavy quarks) are implemented on a set of ensembles

Collaboration	Ref.	N_f	publication status	continuum extrapolation	chiral extrapolation	finite volume	renormalization/matching	heavy-quark treatment	f_D	f_{D_s}	f_{D_s}/f_D
ETM 21B	[5]	2+1+1	C	★	★	★	★	✓	210.1(2.4)	248.9(2.0)	1.1838(115)
FNAL/MILC 17 $^{\nabla\nabla}$	[6]	2+1+1	A	★	★	★	★	✓	212.1(0.6)	249.9(0.5)	1.1782(16)
FNAL/MILC 14A**	[7]	2+1+1	A	★	★	★	★	✓	212.6(0.4) $\binom{+1.0}{-1.2}$	249.0(0.3) $\binom{+1.1}{-1.5}$	1.1745(10) $\binom{+29}{-32}$
ETM 14E	[8]	2+1+1	A	★	○	○	★	✓	207.4(3.8)	247.2(4.1)	1.192(22)
ETM 13F	[9]	2+1+1	C	○	○	○	★	✓	202(8)	242(8)	1.199(25)
FNAL/MILC 13	[10]	2+1+1	C	★	★	★	★	✓	212.3(0.3)(1.0)	248.7(0.2)(1.0)	1.1714(10)(25)
FNAL/MILC 12B	[11]	2+1+1	C	★	★	★	★	✓	209.2(3.0)(3.6)	246.4(0.5)(3.6)	1.175(16)(11)
RQCD/ALPHA 24	[12]	2+1	P	★	★	★	★	✓	208.4(0.7)(0.7)(1.1)	246.8(0.6)(0.6)(1.0)	1.1842(21)(22)(19)
ALPHA 23	[13]	2+1	A	★	○	★	★	✓	211.3(1.9)(0.6)	247.0(1.9)(0.7)	1.177(15)(5)
χQCD 20A††	[14]	2+1	A	■	★	★	★	✓	213(5)	249(7)	1.16(3)
RBC/UKQCD 18A$^{\square\nabla}$	[15]	2+1	P	★	★	★	★	✓			1.1740(51) $\binom{+68}{-68}$
RBC/UKQCD 17	[16]	2+1	A	★	★	○	★	✓	208.7(2.8) $\binom{+2.1}{-1.8}$	246.4(1.3) $\binom{+1.3}{-1.9}$	1.1667(77) $\binom{+57}{-43}$
χQCD 14$^{\dagger\square}$	[17]	2+1	A	○	○	○	★	✓		254(2)(4)	
HPQCD 12A	[18]	2+1	A	○	○	○	★	✓	208.3(1.0)(3.3)	246.0(0.7)(3.5)	1.187(4)(12)
FNAL/MILC 11	[19]	2+1	A	○	○	○	○	✓	218.9(11.3)	260.1(10.8)	1.188(25)
PACS-CS 11	[20]	2+1	A	■	★	■	○	✓	226(6)(1)(5)	257(2)(1)(5)	1.14(3)
HPQCD 10A	[21]	2+1	A	★	○	★	★	✓	213(4)*	248.0(2.5)	
HPQCD/UKQCD 07	[22]	2+1	A	○	○	○	★	✓	207(4)	241 (3)	1.164(11)
FNAL/MILC 05	[23]	2+1	A	○	○	■	○	✓	201(3)(17)	249(3)(16)	1.24(1)(7)

* This result is obtained by using the central value for f_{D_s}/f_D from HPQCD/UKQCD 07 and increasing the error to account for the effects from the change in the physical value of r_1.
** At $\beta = 5.8$, $m_{\pi,\min}L = 3.2$ but this lattice spacing is not used in the final cont./chiral extrapolations.
$^{\nabla\nabla}$ Update of FNAL/MILC 14A. The ratio quoted is $f_{D_s}/f_{D^+} = 1.1749(16)$. In order to compare with results from other collaborations, we rescale the number by the ratio of central values for f_{D^+} and f_D. We use the same rescaling in FNAL/MILC 14A. At the finest lattice spacing the finite-volume criterium would produce an empty green circle, however, as checked by the authors, results would not significantly change by excluding this ensemble, which instead sharpens the continuum limit extrapolation.
$\square\nabla$ Update of RBC/UKQCD 17.
$\dagger\square$ Two values of sea pion masses.
$\dagger\dagger$ Four valence pion masses between 208 MeV and 114 MeV have been used at one value of the sea pion mass of 139 MeV.

Table 28: Decay constants of the D and D_s mesons (in MeV) and their ratio.

of configurations generated within the CLS initiative using $\mathcal{O}(a)$-improved Wilson fermions. As a consequence of the maximal twist, observables in the charm sector are free from $\mathcal{O}(am_c)$ discretisation effects. In addition the decay constants $f_{D_{(s)}}$ are automatically normalized and do not require the computation of normalization factors. Four different lattice spacings have been used in the continuum extrapolation, ranging between 0.087 and 0.05 fm. Pion masses

reach down to 200 MeV and volumes are such that $3.9 \leq m_\pi L \leq 6.4$. The uncertainties are dominated by statistics and the chiral-continuum fits. Judging from the plots in Ref. [13], the values for $\delta(a_{\rm min})$ are around 1 for f_D and around 3 for f_{D_s}.

A second new computation with $N_f = 2+1$ has been performed by the RQCD-ALPHA Collaboration [12] on a set of 49 gauge ensembles generated again within the CLS effort. For this reason statistical errors between ALPHA 23 and RQCD/ALPHA 24 will be treated as 100% correlated when performing averages. Notice, however, that since RQCD/ALPHA 24 was not yet published in a journal by the FLAG deadline, it is not being considered in the averages for this review. In RQCD/ALPHA 24 nonperturbatively $\mathcal{O}(a)$-improved Wilson fermions have been used both in the valence sector and the sea.[1] The simulations cover six different lattice spacings with 0.039 fm $\leq a \leq$ 0.098 fm, pion masses from 420 MeV down to 130 MeV and $m_\pi L$ ranging from 2.83 to 6.42. The largest volume at $m_\pi = 130$ MeV gives $m_\pi L = 4.05$. In the discussion of the final errors the uncertainty due to the scale setting is treated separately. That turns out to be the largest contribution to the total error for f_D and f_{D_s} (around 50%), while for the ratio of decay constants statistical, systematic (chiral and continuum extrapolations) and scale-setting uncertainties are of about the same size. The quantity $\delta(a_{\rm min})$, as estimated from the figures in [12] is around 1.

The updated $N_f = 2+1$ FLAG averages read

$$N_f = 2+1: \qquad f_D = 210.4(1.5)\ \text{MeV} \qquad \text{Refs. [13, 16, 18, 19]}, \tag{126}$$

$$N_f = 2+1: \qquad f_{D_s} = 247.7(1.2)\ \text{MeV} \qquad \text{Refs. [13, 16, 17, 19, 21]}, \tag{127}$$

$$N_f = 2+1: \qquad \frac{f_{D_s}}{f_D} = 1.174(0.007) \qquad \text{Refs. [13, 16, 18, 19]}. \tag{128}$$

Those come from the results in HPQCD 12A [18], FNAL/MILC 11 [19] as well as RBC/UKQCD 17 [16] and ALPHA 23 [13] concerning f_D while for f_{D_s} also the χQCD 14 [17] result contributes, and instead of the value in HPQCD 12A [18] the one in HPQCD 10A [21] is used. In addition, the statistical errors between the results of FNAL/MILC and HPQCD have been everywhere treated as 100% correlated since the two collaborations use overlapping sets of configurations. The same procedure had been used in the past reviews. Concerning the values of $\delta(a_{\rm min})$ for older computations entering those estimates, they are all smaller than 2 for the results before 2013, as discussed in the second FLAG review [4], where that was used as a necessary condition to enter the averages. For RBC/UKQCD 17 $\delta(a_{\rm min})$ is estimated to be around 1.5, while for χQCD 14 it is not possible to assess the value of $\delta(a_{\rm min})$ from the published figures and tables.

For $N_f = 2+1+1$ only a Proceedings contribution to the 2021 Lattice Conference by the ETM Collaboration [5] appeared containing new results. This ETM 21B result extends ETM 14E [8] by including simulations closer to the physical point for light and heavy quarks. Twisted-mass fermions at maximal twist are used in the sea, in order to ensure automatic $\mathcal{O}(a)$ improvement. In the valence sector Osterwalder-Seiler fermions are adopted for the strange and charm quarks to avoid mixing effects at $\mathcal{O}(a^2)$. Three different lattice resolutions between 0.095 fm and 0.069 fm have been used with $m_\pi L$ at the lightest pion mass (134 MeV) being around 3.7. Also in this case the final errors are dominated by statistics and the chiral-continuum extrapolations. Although we do not provide an estimate of $\delta(a_{\rm min})$ for results that do not enter the final averages, ETM 21B makes an important observation in

[1] The coefficient $\bar{b}_{\rm A}$ has been neglected because its nonperturbative value, computed in [24], turned out to be compatible with zero for the relevant range of gauge couplings.

showing that the cutoff effects strongly depend on the intermediate scaling variable used. In the case of f_{D_s}, when using w_0, $\delta(a_{\min})$ would turn out to be very large, while when using the strange-charm meson mass cutoff effects are much reduced and $\delta(a_{\min})$ is around 1.

Our global averages coincide with those in FLAG 21, Ref. [1], namely

$$N_f = 2+1+1: \qquad f_D = 212.0(0.7)\ \text{MeV} \qquad \text{Refs. [6, 8]}, \tag{129}$$

$$N_f = 2+1+1: \qquad f_{D_s} = 249.9(0.5)\ \text{MeV} \qquad \text{Refs. [6, 8]}, \tag{130}$$

$$N_f = 2+1+1: \qquad \frac{f_{D_s}}{f_D} = 1.1783(0.0016) \qquad \text{Refs. [6, 8]}, \tag{131}$$

where the error on the average of f_D has been rescaled by the factor $\sqrt{\chi^2/\text{dof}} = 1.22$. For the two computations entering the results above $\delta(a_{\min})$ is around 2 at most.

Concerning the inclusion of QED effects, significant progress has been made in the computation of form factors for radiative leptonic decays of D mesons.[2] We do not present results in detail here since they are not yet at the level to be reviewed according to the FLAG criteria, however, such processes are important for two reasons. In the region of soft-photon energies they are needed in order to compute the QED corrections to leptonic decays. In that case they have to be combined with the contributions stemming from virtual exchanges of photons between the meson and the charged lepton, in order to remove infrared divergent terms. For hard photons radiative leptonic decays become important probes of the internal structure of hadrons and therefore of physics Beyond the Standard Model. The form factors appear in the decomposition of the hadronic matrix element

$$H_W^{\alpha r}(k,\mathbf{p}) = \epsilon_\mu^r(k) \int d^4y\, e^{iky}\, \mathrm{T}\langle 0|j_W^\alpha(0) j_{em}^\mu(y)|P(\mathbf{p})\rangle\ , \tag{132}$$

with $\epsilon_\mu^r(k)$ the polarisation vector of the outgoing photon (with momentum k), $\mathbf{p}$ the momentum of the generic pseudoscalar meson P and j_W^α and j_{em}^μ the weak and electromagnetic currents, respectively. Such matrix elements can be extracted from suitable three-point correlation functions that can be computed on an Euclidean lattice. In Ref. [25] a set of numerical methods is explored with the main goals of keeping systematic effects due to contributions from unwanted states under control and of optimizing the signal. The study is performed on a single ensemble with $2+1$ flavours of domain wall fermions, $a \simeq 0.11$ fm and $m_\pi \simeq 340$ MeV.

In Ref. [26], which extends Ref. [27], the form factors for the decay $D_s \to \ell\nu_\ell\gamma$ have been computed on four different ensembles of $N_f = 2+1+1$ gauge configurations produced by the ETM Collaboration. Lattice spacings span the interval $[0.056, 0.09]$ fm and quarks masses are close to their physical values. The full kinematical range, with a cut $E_\gamma \geq 10$ MeV, is covered by the results. The structure-dependent contribution is found to dominate the amplitude for $\ell = e$, as opposed to the cases with $\ell = \mu$ and τ. Since the point-like contribution is (helicity) suppressed by $(m_\ell/m_P)^2$, a nonperturbative computation of the form factors is of paramount importance for B mesons. An analysis of the noise-to-signal ratio for the three-point functions is presented following the Parisi-Lepage approach [28, 29] and a strategy to mitigate the problem is discussed. That coincides with one of the methods studied, with different motivations, in Ref. [25].

[2] The accuracy of the estimates presented here is often below the percent level and a first-principles computation of isospin-breaking corrections is therefore very desirable. However, for the determination of the CKM matrix elements, the experimental accuracy on the branching ratios and hence on the products $|V_{cq}|^2 f^2_{D_{(q)}}$ varies between 2.2% and 5%, see section 7.5.

7.2 Form factors for $D \to \pi\ell\nu$ and $D \to K\ell\nu$ semileptonic decays

The SM prediction for the differential decay rate of the semileptonic processes $D \to \pi\ell\nu$ and $D \to K\ell\nu$ can be written as

$$\frac{d\Gamma(D \to P\ell\nu)}{dq^2} = \frac{\eta_{\rm EW}^2 G_{\rm F}^2 |V_{cx}|^2}{24\pi^3} \frac{(q^2 - m_\ell^2)^2 \sqrt{E_P^2 - m_P^2}}{q^4 m_D^2} \times \left[\left(1 + \frac{m_\ell^2}{2q^2}\right) m_D^2 (E_P^2 - m_P^2) |f_+(q^2)|^2 + \frac{3m_\ell^2}{8q^2} (m_D^2 - m_P^2)^2 |f_0(q^2)|^2 \right] \tag{133}$$

where $x = d, s$ is the daughter light quark, $P = \pi, K$ is the daughter light-pseudoscalar meson, $\ell = e, \mu$ indicates the light charged lepton, E_P is the light-pseudoscalar meson energy in the rest frame of the decaying D, and $q = (p_D - p_P)$ is the momentum of the outgoing lepton pair. Here, we have included the short-distance electroweak correction factor [30], whose value at $\mu = m_D$ is $\eta_{\rm EW} = 1.009$ [31]. The vector and scalar form factors $f_+(q^2)$ and $f_0(q^2)$ parameterize the hadronic matrix element of the heavy-to-light quark flavour-changing vector current $V_\mu = \bar{x}\gamma_\mu c$,

$$\langle P|V_\mu|D\rangle = f_+(q^2) \left(p_{D\mu} + p_{P\mu} - \frac{m_D^2 - m_P^2}{q^2} q_\mu \right) + f_0(q^2) \frac{m_D^2 - m_P^2}{q^2} q_\mu \,, \tag{134}$$

and satisfy the kinematic constraint $f_+(0) = f_0(0)$. Because the contribution to the decay width from the scalar form factor is proportional to m_ℓ^2, within current precision standards it can be neglected for $\ell = e$, and Eq. (133) simplifies to

$$\frac{d\Gamma(D \to Pe\nu)}{dq^2} = \frac{\eta_{\rm EW}^2 G_{\rm F}^2}{24\pi^3} |\vec{p}_P|^3 |V_{cx}|^2 |f_+(q^2)|^2 \,. \tag{135}$$

In models of new physics, decay rates may also receive contributions from matrix elements of other parity-even currents. In the case of the scalar density $(\bar{x}c)$, partial vector-current conservation allows one to write its matrix elements in terms of f_+ and f_0, while for tensor currents $T_{\mu\nu} = \bar{x}\sigma_{\mu\nu}c$ a new form factor has to be introduced, viz.,

$$\langle P|T^{\mu\nu}|D\rangle = \frac{2}{m_D + m_P} \left[p_P^\mu p_D^\nu - p_P^\nu p_D^\mu \right] f_T(q^2) \,. \tag{136}$$

Recall that, unlike the Noether current V_μ, the operator $T_{\mu\nu}$ requires a scale-dependent renormalization.

Lattice-QCD computations of $f_{+,0}$ allow for comparisons to experiment to ascertain whether the SM provides the correct prediction for the q^2-dependence of $d\Gamma(D \to P\ell\nu)/dq^2$; and, subsequently, to determine the CKM matrix elements $|V_{cd}|$ and $|V_{cs}|$ from Eq. (133). The inclusion of f_T allows for analyses to constrain new physics. Currently, state-of-the-art experimental results by CLEO-c [32] and BESIII [33, 34] provide data for the differential rates in the whole q^2 range, with a precision of order 2–3% for the total branching fractions in both the electron and muon final channels.

Calculations of the $D \to \pi\ell\nu$ and $D \to K\ell\nu$ form factors typically use the same light-quark and charm-quark actions as those of the leptonic decay constants f_D and f_{D_s}. Therefore, many of the same issues arise; in particular, considerations about cutoff effects coming from the large charm-quark mass, or the normalization of weak currents, apply. Additional complications arise, however, due to the necessity of covering a sizeable range of values in q^2:

- Lattice kinematics impose restrictions on the values of the hadron momenta. Because lattice calculations are performed in a finite spatial volume, the pion or kaon three-momentum components can only take discrete values in units of $2\pi/L$ when periodic boundary conditions are used. For typical box sizes in lattice D- and B-meson form-factor calculations at heavier-than-physical pion masses, $L \sim 2.5$–3 fm; thus, the smallest nonzero momentum in most of these analyses is $|\vec{p}_P| \sim 400$–500 MeV. On the other hand, the ranges relevant for the semileptonic decays are $0 \leq |\vec{p}_\pi| \lesssim 940$ MeV and $0 \leq |\vec{p}_K| \lesssim 1$ GeV, respectively. Thus, when using periodic boundary conditions, only a small number of allowed lattice momenta fall into this range. As a consequence, many studies have incorporated the use of nonperiodic "twisted" boundary conditions (tbc) [35, 36] in the valence fields used for the computation of observables, which allows a continuous choice of momentum and hence finer resolution of the q^2-dependence [37–42]. Note that more recent calculations [31, 43] include ensembles with physical pion masses and $L \approx 5.5$–5.75 fm, so the momentum unit when using periodic boundary conditions is correspondingly smaller, making the use of twisted boundary conditions less relevant.

- Final-state pions and kaons can have energies $\gtrsim 1$ GeV, given the available kinematical range $0 \lesssim q^2 \leq q^2_{\rm max} = (m_D - m_P)^2$. This makes the use of (heavy-meson) chiral perturbation theory to extrapolate to physical light-quark masses potentially problematic. This issue has become less relevant as modern calculations include ensembles with physical light-quark masses.

- Accurate comparisons to experiment, including the determination of CKM parameters, requires good control of systematic uncertainties in the parameterization of the q^2-dependence of form factors. While this issue is far more important for semileptonic B decays, where it is harder to cover the kinematic range on the lattice, the increase in experimental precision requires accurate work in the charm sector as well. The parameterization of semileptonic form factors is discussed in detail in Appendix B.2.

The first published $N_f = 2{+}1$ lattice-QCD calculation of the $D \to \pi\ell\nu$ and $D \to K\ell\nu$ form factors came from the Fermilab Lattice, MILC, and HPQCD collaborations (FNAL/MILC 04) [44].[3] This work uses asqtad-improved staggered sea quarks and light (u, d, s) valence quarks and the Fermilab action for the charm quarks, with a single lattice spacing of $a \approx 0.12$ fm, and a minimum RMS-pion mass of ≈ 510 MeV, dictated by the presence of fairly large staggered taste splittings. The vector current is normalized using a mostly nonperturbative approach, such that the perturbative truncation error is expected to be negligible compared to other systematics. Results for the form factors are provided over the full kinematic range, rather than focusing just at $q^2 = 0$ as was customary in most previous work, and fitted to a Bečirević-Kaidalov ansatz (calculations in the full kinematic range had already been done earlier in the quenched approximation [45, 46]). The publication of Ref. [44] predated the precise measurements of the $D \to K\ell\nu$ decay width by the FOCUS [47] and Belle experiments [48], and showed good agreement with the experimental determination of the shape of $f_+^{D\to K}(q^2)$. Progress on extending this work was reported in [49]; efforts are aimed at reducing both the statistical and systematic errors in $f_+^{D\to\pi}(q^2)$ and $f_+^{D\to K}(q^2)$ by increasing the number of

[3] Because only two of the authors of this work are members of HPQCD, and to distinguish it from other more recent works on the same topic by HPQCD, we hereafter refer to this work as "FNAL/MILC."

configurations analyzed, simulating with lighter pions, and adding lattice spacings as fine as $a \approx 0.045$ fm.

The most precise published calculations of the $D \to \pi\ell\nu$ and $D \to K\ell\nu$ form factors in $N_f = 2+1$ QCD are by the HPQCD collaboration (HPQCD 11 [50] and HPQCD 10B [51], respectively). They are also based on $N_f = 2+1$ asqtad-improved staggered MILC configurations, but use two lattice spacings $a \approx 0.09$ and 0.12 fm, and a HISQ action for the valence u, d, s, and c quarks. In these mixed-action calculations, the HISQ valence light-quark masses are tuned so that the ratio m_l/m_s is approximately the same as for the sea quarks; the minimum RMS sea-pion mass ≈ 390 MeV. Form factors are determined only at $q^2 = 0$, by using a Ward identity to relate matrix elements of vector currents to matrix elements of the absolutely normalized quantity $(m_c - m_x)\langle P|\bar{x}c|D\rangle$ (where $x = u, d, s$), and exploiting the kinematic identity $f_+(0) = f_0(0)$ to yield $f_+(q^2 = 0) = (m_c - m_x)\langle P|\bar{x}c|D\rangle/(m_D^2 - m_P^2)$. A modified z-expansion (cf. Appendix B.2) is employed to simultaneously extrapolate to the physical light-quark masses and the continuum and to interpolate to $q^2 = 0$, and allow the coefficients of the series expansion to vary with the light- and charm-quark masses. The form of the light-quark dependence is inspired by χPT, and includes logarithms of the form $m_\pi^2 \log(m_\pi^2)$ as well as polynomials in the valence-, sea-, and charm-quark masses. Polynomials in $E_{\pi(K)}$ are also included to parameterize momentum-dependent discretization errors. The number of terms is increased until the result for $f_+(0)$ stabilizes, such that the quoted fit error for $f_+(0)$ not only contains statistical uncertainties, but also reflects relevant systematics. The largest quoted uncertainties in these calculations are from statistics and charm-quark discretization errors.

The most recent $N_f = 2+1$ computation of D semileptonic form factors has been carried out by the JLQCD collaboration, and so far only published in conference proceedings; most recently in Ref. [52] (JLQCD 17B). They use their own Möbius domain-wall configurations at three values of the lattice spacing $a = 0.080, 0.055, 0.044$ fm, with several pion masses ranging from 226 to 501 MeV (though there is so far only one ensemble, with $m_\pi = 284$ MeV, at the finest lattice spacing). The vector and scalar form factors are computed at four values of the momentum transfer for each ensemble. The computed form factors are observed to depend mildly on both the lattice spacing and the pion mass. The momentum dependence of the form factors is fitted to a BCL z-parameterization (see Appendix B.2) with a Blaschke factor that contains the measured value of the $D^*_{(s)}$ mass in the vector channel, and a trivial Blaschke factor in the scalar channel. The systematics of this latter fit is assessed by a BCL fit with the experimental value of the scalar resonance mass in the Blaschke factor. Continuum and chiral extrapolations are carried out through a linear fit in the squared lattice spacing and the squared pion and η_c masses. A global fit that uses hard-pion HMχPT to model the mass dependence is furthermore used for a comparison of the form factor shapes with experimental data.[4] Since the computation is only published in proceedings so far, it will not enter our $N_f = 2+1$ average.[5] Another $N_f = 2+1$ calculation of the $D \to \pi$, $D \to K$, and $D_s \to K$ form factors using domain-wall fermions is currently being carried out by the RBC/UKQCD

[4] It is important to stress the finding in Ref. [53] that the factorization of chiral logs in hard-pion χPT breaks down, implying that it does not fulfill the expected requisites for a proper effective field theory. Its use to model the mass dependence of form factors can thus be questioned.

[5] The ensemble parameters quoted in Ref. [52] appear to show that the volumes employed at the lightest pion masses are insufficient to meet our criteria for finite-volume effects. There is, however, a typo in the table which results in a wrong assignment of lattice sizes, whereupon the criteria are indeed met. We thank T. Kaneko for correspondence on this issue.

collaboration, as reported in Ref. [54].

The first full computation of both the vector and scalar form factors in $N_f = 2+1+1$ QCD was achieved by the ETM collaboration [41] (ETM 17D). Furthermore, they have provided a separate determination of the tensor form factor, relevant for new-physics analyses [42] (ETM 18). Both works use the available $N_f = 2+1+1$ twisted-mass Wilson ensembles [55], totaling three lattice spacings down to $a \approx 0.06$ fm, and a minimum pion mass of 220 MeV. Matrix elements are extracted from suitable double ratios of correlation functions that avoid the need of nontrivial current normalizations. Only one source-sink separation per ensemble is used for the three-point functions, although the authors state that this separation was optimized to achieve a balance between excited-state contamination and statistical uncertainties. The use of twisted boundary conditions allows both for imposing several kinematical configurations, and considering arbitrary frames that include moving initial mesons. After interpolation to the physical strange- and charm-quark masses, the results for form factors are fitted to a modified z-expansion that takes into account both the light-quark mass dependence through hard-pion SU(2) χPT [56], and the lattice-spacing dependence. In the latter case, a detailed study of Lorentz-breaking effects due to the breaking of rotational invariance down to the hypercubic subgroup is performed, leading to a nontrivial momentum-dependent parameterization of cutoff effects. The z-parameterization (see Appendix B.2) itself includes a single-pole Blaschke factor (save for the scalar channel in $D \to K$, where the Blaschke factor is trivial), with pole masses treated as free parameters. The final quoted uncertainty on the form factors is about 5–6% for $D \to \pi$, and 4% for $D \to K$. The dominant source of uncertainty is quoted as statistical+fitting procedure+input parameters — the latter referring to the values of quark masses, the lattice spacing (i.e., scale setting), and the LO SU(2) LECs.

The second $N_f = 2+1+1$ computation of f_+ and f_0 in the full kinematical range for the $D \to Kl\nu$ mode, performed by HPQCD, has been published in 2021 — HPQCD 21A (Ref. [43]). This work uses MILC's HISQ ensembles at five values of the lattice spacing, and pion masses reaching to the physical point for the three coarsest values of a. Vector currents are normalized nonpertubatively by imposing that form factors satisfy Ward identities exactly at zero recoil. Results for the form factors are fitted to a modified z-expansion ansatz, with all sub-threshold poles removed by using the experimental value of the mass shifted by a factor that matches the corresponding result at finite lattice spacing. The accuracy of the description of the q^2-dependence is crosschecked by comparing to a fit based on cubic splines. Finite-volume effects are expected to be small, and chiral-perturbation-theory-based estimates for them are included in the chiral fit. The impact of frozen topology at the finest lattice spacing is neglected (the size of this effect was later shown to be $\lesssim 0.03\%$ in a similar calculation [31]). The final uncertainty from the form factors in the determination of $|V_{cs}|$ quoted in HPQCD 21A is at the 0.5% level, and comparable to the rest of the uncertainty (due to the experimental error, as well as weak and electromagnetic corrections); in particular, the precision of the form factors is around seven times higher than that of the earlier $N_f = 2+1+1$ determination by ETM 17D. The work also provides an accurate prediction for the lepton-flavour-universality ratio between the muon and electron modes, where the uncertainty is overwhelmingly dominated by the electromagnetic corrections. An extension of the work of HPQCD 21A to heavier quark masses has also enabled the determination of the $B \to K$ form factors [57] (HPQCD 22), and provides the tensor form factors for both $B \to K$ and $D \to K$ in addition to the vector form factors.

In 2022, the FNAL/MILC collaboration completed another $N_f = 2+1+1$ computation of f_+ and f_0 in the full kinematic ranges for $D \to K\ell\nu$, $D \to \pi\ell\nu$, and $D_s \to Kl\nu$ –

FNAL/MILC 22 [31]. Like HPQCD 21A, this calculation uses the MILC HISQ ensembles and renormalization using the vector Ward identity. This calculation does not include the 0.15 fm ensembles that were part of the HPQCD 21A analysis, and shares only one of the two 0.12 fm ensembles used in HPQCD 21A. Compared to HPQCD 21A, FNAL/MILC 22 reaches a finer lattice spacing at the physical pion mass, 0.057 fm, while the ensemble at the finest lattice spacing of 0.042 fm is common to both calculations. Overall, four of the seven ensembles are shared, but FNAL/MILC 22 uses more configurations and source positions on those ensembles. In FNAL/MILC 22, the chiral/continuum extrapolation is performed using rooted staggered heavy-meson chiral perturbation theory prior to a continuum BCL z expansion fit. This work also corrects the effects of the frozen topology at the finest lattice spacing using chiral perturbation theory; the correction is found to be $\lesssim 0.03\%$.

Collaboration	Ref.	N_f	publication status	continuum extrapolation	chiral extrapolation	finite volume	renormalization	heavy-quark treatment	$f_+^{D\to\pi}(0)$	$f_+^{D\to K}(0)$
FNAL/MILC 22	[31]	2+1+1	A	★	★	★	★	✓	0.6300(51)	0.7452(31)
HPQCD 22	[57]	2+1+1	A	★	★	★	★	✓	n/a	0.7441(40)
HPQCD 21A	[43]	2+1+1	A	★	★	★	★	✓	n/a	0.7380(44)
HPQCD 20	[58]	2+1+1	A	★	○	★	★	✓	n/a	n/a
ETM 17D, 18	[41, 42]	2+1+1	A	★	○	○	★	✓	0.612(35)	0.765(31)
JLQCD 17B	[52]	2+1	C	★	★	○	★	✓	$0.615(31)(^{+17}_{-16})(^{+28}_{-7})^*$	$0.698(29)(18)(^{+32}_{-12})^*$
HPQCD 11	[50]	2+1	A	○	○	○	★	✓	0.666(29)	
HPQCD 10B	[51]	2+1	A	○	○	○	★	✓		0.747(19)
FNAL/MILC 04	[44]	2+1	A	■	■	○	○	✓	0.64(3)(6)	0.73(3)(7)

* The first error is statistical, the second from the $q^2 \to 0$ extrapolation, the third from the chiral-continuum extrapolation.

Table 29: Summary of computations of charmed-meson semileptonic form factors. Note that HPQCD 20 (discussed in Sec. 7.4) addresses the $B_c \to B_s$ and $B_c \to B_d$ transitions—hence the absence of quoted values for $f_+^{D\to\pi}(0)$ and $f_+^{D\to K}(0)$—while ETM 18 and HPQCD 22 provide computations of tensor form factors. The value for $f_+^{D\to K}(0)$ from HPQCD 22 [57] is obtained as a by-product of the $B \to K$ analysis and is not independent from HPQCD 21A [43]. FNAL/MILC 22 also provides results for the $D_s \to K$ form factors in addition to the $D \to K$ and $D \to \pi$ form factors [31].

Table 29 contains our summary of the existing calculations of the charm-meson semileptonic form factors. Additional tables in Appendix C.4.1 provide further details on the simulation parameters and comparisons of the error estimates. Recall that only calculations without red tags that are published in a refereed journal are included in the FLAG

average. For $N_f = 2+1$, only HPQCD 10B,11 qualify, which provides our estimate for $f_+(q^2=0) = f_0(q^2=0)$. For $N_f = 2+1+1$, we quote as the FLAG estimate for $f_+^{D\to\pi}(0)$ the weighted average of the results by ETM 17D and FNAL/MILC 22, while for $f_+^{D\to K}(0)$ we quote the weighted average of the values published by ETM 17D, HPQCD 21A, and FNAL/MILC 22:

$$N_f = 2+1: \quad \begin{array}{ll} f_+^{D\to\pi}(0) = 0.666(29) & \text{Ref. [50]}, \\ f_+^{D\to K}(0) = 0.747(19) & \text{Ref. [51]}, \end{array} \tag{137}$$

$$N_f = 2+1+1: \quad \begin{array}{ll} f_+^{D\to\pi}(0) = 0.6296(50) & \text{Refs. [31, 41]}, \\ f_+^{D\to K}(0) = 0.7430(27) & \text{Refs. [31, 41, 43]}. \end{array} \tag{138}$$

In Fig. 17, we display the existing $N_f = 2$, $N_f = 2+1$, and $N_f = 2+1+1$ results for $f_+^{D\to\pi}(0)$ and $f_+^{D\to K}(0)$; the grey bands show our estimates of these quantities.

In the case of $N_f = 2+1+1$, we can also provide an analysis of the q^2-dependence of f_+ and f_0. FLAG 21 included a BCL fit to the ETM 17D and HPQCD 21 results for the $D\to K$ form factors; this fit had a relatively poor $\chi^2/\text{dof} = 9.17/3$ due to a tension between the results from the two collaborations at large q^2; for $D\to\pi$, only the ETM 17D results were available at that time. Now, the FNAL/MILC 22 calculation [31] provides new high-precision $N_f = 2+1+1$ results for both $D\to K$ and $D\to\pi$ (as well as $D_s\to K$). For $D\to K$, we update our previous BCL fit to include the FNAL/MILC 22 results. We consider the statistical correlations between the final HPQCD 21A and FNAL/MILC 22 results to be negligible, given that there is only partial overlap among the ensembles, the source positions for the correlation functions are different, and the analyses are performed with different fit methodologies. As in FLAG 21, we generate synthetic data from the parameterizations provided by the collaborations. The inputs to our fit from ETM 17D and HPQCD 21A are unchanged; for FNAL/MILC 22 we use four q^2 values because the parameterization used in that reference is of higher order. In both cases, this includes the kinematical endpoints $q^2 = 0$ and $q^2 = (m_D - m_K)^2$ of the semileptonic interval. We fit the resulting dataset to a BCL ansatz (cf. Eqs. (527) and (528)); the constraint $f_+(0) = f_0(0)$ is used to rewrite the highest-order coefficient $a^0_{N_0-1}$ in f_0 in terms of the other $N_+ + N_0 - 1$ coefficients. In both form factors, we include nontrivial Blaschke factors, with pole masses set to the experimental values of the D_s^* (for the vector channel) and D_{s0}^* (scalar channel) masses found in the PDG [59]. We take flavour averages of charged and neutral states for the D and K masses. Our external input is thus $m_D = 1.87265$ GeV, $m_K = 495.644$ MeV, $m_{D_s^*} = 2.1122$ GeV, and $m_{D_{s0}^*} = 2.317$ GeV. As a result of including the new FNAL/MILC 22 data points, we found it necessary to increase the order of the z expansion from $N_+ = N_0 = 3$ (as used in FLAG 21) to $N_+ = N_0 = 4$. The fit has $\chi^2/\text{dof} \approx 2.39$ (due to the tension between the ETM 17D results at high q^2 and the results from the other two collaborations, and due to a slight tension between the results from HPQCD 21A and FNAL/MILC 22 in f_0) and we have scaled the uncertainties of all parameters by a factor of $\sqrt{\chi^2/\text{dof}} \approx 1.55$. The results are quoted in full in Tab. 30 and illustrated in Fig. 18.

As can be seen in Fig. 19 of Ref. [31], for $D\to\pi$ there is a very large tension between the ETM 17D and FNAL/MILC 22 results at high q^2, in the same direction as the tension

$D \to K\ell\nu$ ($N_f = 2+1+1$)

	values	correlation matrix						
a_0^+	0.7953(53)	1.	−0.690759	−0.051101	−0.061092	0.501293	0.469810	0.132470
a_1^+	−1.0090(87)	−0.690759	1.	−0.231861	0.133663	0.004097	0.149657	0.137516
a_2^+	0.22(59)	−0.051101	−0.231861	1.	−0.113075	−0.095636	0.101738	0.238861
a_3^+	0.14(10)	−0.061092	0.133663	−0.113075	1.	−0.109883	0.116543	0.112918
a_0^0	0.7026(21)	0.501293	0.004097	−0.095636	−0.109883	1.	0.339786	−0.251322
a_1^0	0.773(39)	0.469810	0.149657	0.101738	0.116543	0.339786	1.	0.589149
a_2^0	0.54(40)	0.132470	0.137516	0.238861	0.112918	−0.251322	0.589149	1.

Table 30: Coefficients for the $N^+ = 4, N^0 = 4$ z-expansion of the $N_f = 2+1+1$ FLAG average for the $D \to K$ form factors f_+ and f_0, and their correlation matrix. The inputs are from ETM 17D, HPQCD 21A, and FNAL/MILC 22. The form factors can be reconstructed using parameterization and inputs given in Appendix B.3.1.

also seen for $D \to K$. In this case, the tension is so significant that attempting BCL fits to average the ETM 17D and FNAL/MILC 22 results gives values of χ^2/dof of order 100. We are concerned about possible excited-state contamination in ETM 17D, but the authors of ETM 17D stated that there is no evidence of an uncontrolled systematic effect; the tension remains unexplained. We therefore do not quote any results for the $D \to \pi$ form factors away from $q^2 = 0$.

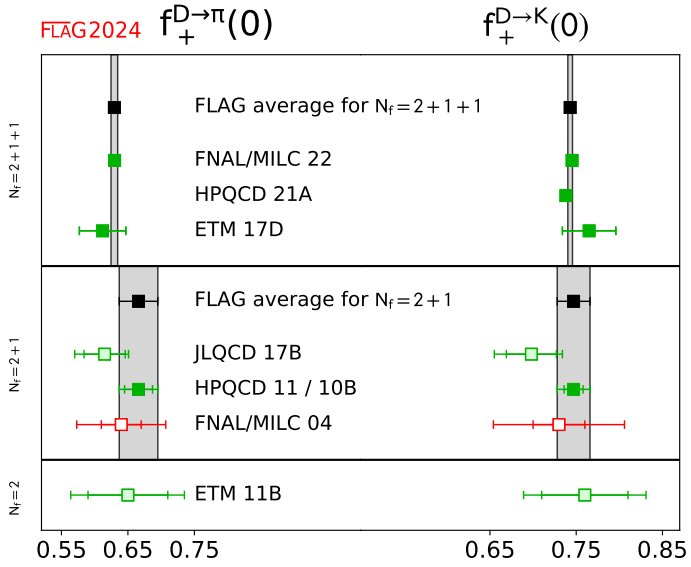

Figure 17: $D \to \pi\ell\nu$ and $D \to K\ell\nu$ semileptonic form factors at $q^2 = 0$. The $N_f = 2+1$ HPQCD result for $f_+^{D\to\pi}(0)$ is from HPQCD 11, the one for $f_+^{D\to K}(0)$ represents HPQCD 10B (see Tab. 29).

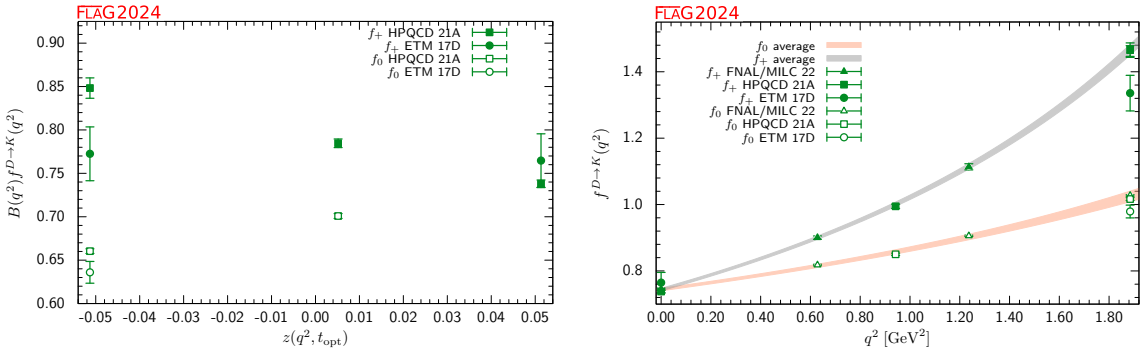

Figure 18: The form factors $f_+(q^2)$ and $f_0(q^2)$ for $D \to K\ell\nu$ plotted versus z (left panel) and q^2 (right panel). In the left plot, we removed the Blaschke factors. See text for a discussion of the data set. The grey and salmon bands display our preferred $N^+ = N^0 = 4$ BCL fit (seven parameters).

7.3 Form factors for Λ_c and Ξ_c semileptonic decays

The motivation for studying charm-baryon semileptonic decays is two-fold. First, these decays allow for independent determinations of $|V_{cs}|$. Second, given that possible new-physics contributions to the $c \to s\ell\nu$ weak effective Hamiltonian are already constrained to be much smaller compared to $b \to u\ell\bar{\nu}$ and $b \to s\ell\ell$, charm-baryon semileptonic decays allow testing the lattice techniques for baryons that are also employed for bottom-baryon semileptonic decays (see Sec. 8.6) in a better-controlled environment.

The amplitudes of the decays $\Lambda_c \to \Lambda\ell\nu$ receive contributions from both the vector and the axial components of the current in the matrix element $\langle\Lambda|\bar{s}\gamma^\mu(\mathbf{1}-\gamma_5)c|\Lambda_c\rangle$, and can be parameterized in terms of six different form factors f_+, f_0, $f_\perp$, g_+, g_0, $g_\perp$ — see, e.g., Ref. [60] for a complete description.

The computation in Meinel 16 [61] uses RBC/UKQCD $N_f = 2+1$ DWF ensembles, and treats the c quarks within the Columbia RHQ approach. Two values of the lattice spacing ($a \approx 0.11,\ 0.085$ fm) are considered, with the absolute scale set from the $\Upsilon(2S)$–$\Upsilon(1S)$ splitting. In one ensemble, the pion mass $m_\pi \approx 139$ MeV is at the physical point, while for other ensembles it ranges from 295 to 352 MeV. Results for the form factors are obtained from suitable three-point functions, and fitted to a modified z-expansion ansatz that combines the q^2-dependence with the chiral and continuum extrapolations. The paper predicts for the total rates in the e and μ channels

$$\begin{aligned}\frac{\Gamma(\Lambda_c \to \Lambda e^+\nu_e)}{|V_{cs}|^2} &= 0.2007(71)(74)\ \text{ps}^{-1}\,,\\ \frac{\Gamma(\Lambda_c \to \Lambda \mu^+\nu_\mu)}{|V_{cs}|^2} &= 0.1945(69)(72)\ \text{ps}^{-1}\,,\end{aligned} \tag{139}$$

where the uncertainties are statistical and systematic, respectively. In combination with the recent experimental determination of the total branching fractions by BESIII [62, 63], it is possible to extract $|V_{cs}|$ as discussed in Sec. 7.5 below.

Lattice results are also available for the $\Lambda_c \to N$ form factors, where N is a neutron or proton [64]. This calculation uses the same lattice actions but a different set of ensembles with parameters matching those used in the 2015 calculation of the $\Lambda_b \to p$ form factors in Ref. [65] (cf. Sec. 8.6). Predictions are given for the rates of the $c \to d$ semileptonic decays $\Lambda_c \to n\ell^+\nu_\ell$; these modes have not yet been observed. Reference [64] also studies the phenomenology of the flavour-changing neutral-current decay $\Lambda_c \to p\mu^+\mu^-$. As is typical for rare charm decays to charged leptons, this mode is dominated by long-distance effects that have not yet been calculated on the lattice and whose description is model-dependent.

The authors of Zhang 21 [66] also performed a first lattice calculation of the $\Xi_c \to \Xi$ form factors and extracted $|V_{cs}|$, with still large uncertainties, from the recent Belle measurement of the $\Xi_c \to \Xi\ell^+\nu_\ell$ branching fractions [67]. This calculation uses only two ensembles with $2+1$ flavours of clover fermions, with lattice spacings of 0.108 and 0.080 fm and nearly identical pion masses of 290 and 300 MeV. The results are extrapolated to the continuum limit but are not extrapolated to the physical pion mass. No systematic uncertainty is estimated for the effect of the missing chiral extrapolation. A new calculation of the $\Xi_c \to \Xi$ form factors using domain-wall fermions is in progress [68].

The calculations discussed so far in this section all have $J^P = \frac{1}{2}^+$ baryons in the final state. A first lattice calculation of the form factors for a charm-baryon semileptonic decay to a $J^P = \frac{3}{2}^-$ baryon, $\Lambda_c \to \Lambda^*(1520)\ell^+\nu_\ell$, is also available: Meinel 21B [69]. The calculation was

done using three RBC/UKQCD ensembles with $2+1$ flavours of domain-wall fermions, with $a \approx 0.11,\ 0.08$ fm and pion masses in the range from approximately 300 to 430 MeV. Chiral-continuum extrapolations linear in m_π^2 and a^2 were performed, with systematic uncertainties estimated using higher-order fits. Finite-volume effects and effects associated with the strong decays of the $\Lambda^*(1520)$ are not quantified. The calculation was done in the $\Lambda^*(1520)$ rest frame, where the cubic symmetry is sufficient to avoid mixing with unwanted lower-mass states.

A summary of the lattice calculations of charm-baryon semileptonic-decay form factors is given in Tab. 31.

Process	Collaboration	Ref.	N_f	publication status	continuum extrapolation	chiral extrapolation	finite volume	renormalization	heavy-quark treatment
$\Lambda_c \to \Lambda^*(1520)\ell\nu$	Meinel 21B	[69]	2+1	A	○	○	■	○	✓
$\Xi_c \to \Xi\ell\nu$	Zhang 21	[66]	2+1	P	○	■	○	★	■
$\Lambda_c \to n\ell\nu$	Meinel 17	[64]	2+1	A	○	○	■	○	✓
$\Lambda_c \to \Lambda\ell\nu$	Meinel 16	[61]	2+1	A	○	★	★	○	✓

Table 31: Summary of computations of charmed-baryon semileptonic form factors. The rationale for the ■ rating of finite-volume effects in Meinel 21B (despite meeting the ○ criterion based on the minimum pion mass) is that the unstable nature of the final-state baryons was neglected in the analysis.

7.4 Form factors for charm semileptonic decays with heavy spectator quarks

Two other decays mediated by the $c \to s\ell\nu$ and $c \to d\ell\nu$ transitions are $B_c \to B_s\ell\nu$ and $B_c \to B^0\ell\nu$, respectively. At present, there are no experimental results for these processes, but it may be possible to produce them at LHCb in the future. The HPQCD Collaboration has recently computed the form factors for both of these B_c decay modes with $N_f = 2+1+1$ [58]. The calculation uses six different MILC ensembles with HISQ light, strange, and charm quarks, and employs the PCAC Ward identity to nonperturbatively renormalize the $c \to s$ and $c \to d$ currents. Data were generated for two different choices of the lattice action for the spectator b quark: lattice NRQCD on five of the six ensembles, and HISQ on three of the six ensembles (cf. Sec. 8 for a discussion of different lattice approaches used for the b quark). For the NRQCD calculation, two of the ensembles have a physical light-quark mass, and the lattice spacings are 0.15 fm, 0.12 fm, and 0.09 fm. The heavy-HISQ calculation is performed only at $m_l/m_s = 0.2$, and at lattice spacings of 0.12 fm, 0.09 fm, and 0.06 fm. The largest value of the heavy-HISQ mass used is 0.8 in lattice units on all three ensembles, which does not reach the physical b-quark mass even at the finest lattice spacing.

Form-factor fits are performed using z-expansions (see Appendix B.2) modified to include a dependence on the lattice spacing and quark masses, including an expansion in the inverse heavy quark mass in the case of the heavy-HISQ approach. The parameters t_+ are set to $(m_{B_c}+m_{B_{(s)}})^2$ even though the branch cuts start at $(m_D+m_K)^2$ or $(m_D+m_\pi)^2$, as also noted by the authors. The variable z is rescaled by a constant. The lowest charmed-meson poles are removed before the z-expansion, but this still leaves the branch cuts and higher poles below t_+. As a consequence of this structure, the good convergence properties of the z-expansion are not necessarily expected to apply. Fits are performed (i) using the NRQCD data only, (ii) using the HISQ data only, and (iii) using the NRQCD data, but with priors on the continuum-limit form-factor parameters equal to the results of the HISQ fit. The results from fits (i) and (ii) are mostly consistent, with the NRQCD fit having smaller uncertainties than the HISQ fit. Case (iii) then results in the smallest uncertainties and gives the predictions (for massless leptons)

$$\begin{aligned}\frac{\Gamma(B_c\to B_s\ell^+\nu_\ell)}{|V_{cs}|^2} &= 1.738(55)\times 10^{-11}\ \text{MeV}\,,\\ \frac{\Gamma(B_c\to B^0\ell^+\nu_\ell)}{|V_{cd}|^2} &= 2.29(12)\times 10^{-11}\ \text{MeV}\,,\\ \frac{\Gamma(B_c\to B_s\ell^+\nu_\ell)|V_{cd}|^2}{\Gamma(B_c\to B^0\ell^+\nu_\ell)|V_{cs}|^2} &= 0.759(44).\end{aligned} \tag{140}$$

We note that there is a discrepancy between the NRQCD and HISQ results in the case of $f_0(B_c\to B^0)$, and the uncertainty quoted for method (iii) does not cover this discrepancy. However, this form factor does not enter in the decay rate for massless leptons.

7.5 Determinations of $|V_{cd}|$ and $|V_{cs}|$ and test of second-row CKM unitarity

We now use the lattice-QCD results for the charm-hadron decays to determine the CKM matrix elements $|V_{cd}|$ and $|V_{cs}|$ in the Standard Model.

For the leptonic decays, we use the latest experimental averages from the Particle Data Group [3] (see Sec. 72.3.1)

$$f_D|V_{cd}| = 45.82(1.10)\ \text{MeV}\,,\qquad f_{D_s}|V_{cs}| = 243.5(2.7)\ \text{MeV}, \tag{141}$$

where the errors include those from nonlattice theory, e.g., estimates of radiative corrections to lifetimes [70]. Also, the values quoted by the Particle Data Group are obtained after applying the correction factor $\eta_{\text{EW}}^2 = 1.018$, due to universal short-distance electroweak contributions [30], to the branching ratios. Hadronic-structure-dependent electromagnetic corrections to the rate have not been computed on the lattice for the case of $D_{(s)}$ mesons, while they have been calculated for pion and kaon decays [71, 72]. The errors given above include a systematic uncertainty of 0.7% estimated as half the size of the applied radiative corrections.

By combining these with the averaged $N_f = 2+1$ and $2+1+1$ results for f_D and f_{D_s} in

Eqs. (126-130), we obtain

$$N_f = 2+1+1\text{:} \quad \begin{cases} |V_{cd}| &= 0.2161(7)(52) \\ |V_{cs}| &= 0.974(2)(11) \end{cases} \qquad [D_{(s)} \to \ell\nu, \text{Refs. [6, 8]}], \tag{142}$$

$$N_f = 2+1\text{:} \quad \begin{cases} |V_{cd}| &= 0.2178(16)(52) \\ |V_{cs}| &= 0.983(5)(11) \end{cases} \qquad [D_{(s)} \to \ell\nu, \text{Refs. [13, 16–19, 21]}], \tag{143}$$

where the errors shown are from the lattice calculation and experiment (plus nonlattice theory), respectively. For the $N_f = 2+1$ and the $N_f = 2+1+1$ determinations, the uncertainties from the lattice-QCD calculations of the decay constants are significantly smaller than the experimental uncertainties in the branching fractions.

For D-meson semileptonic decays, in the case of $N_f = 2+1$ there are no changes with respect to FLAG 21 other than the inclusion of the short-distance electroweak correction and a systematic uncertainty due to missing long-distance QED corrections; the only works entering the FLAG averages are HPQCD 10B/11 [50, 51], which provide $f_+^{D\pi}(0)$ and $f_+^{DK}(0)$. We use these results in combination with the HFLAV averages for the combinations $f_+(0)\eta_{\rm EW}|V_{cx}|$ [73],

$$f_+^{D\pi}(0)\eta_{\rm EW}|V_{cd}| = 0.1426(18)\,, \qquad f_+^{DK}(0)\eta_{\rm EW}|V_{cs}| = 0.7180(33), \tag{144}$$

and obtain

$$N_f = 2+1\text{:}\ |V_{cd}| = 0.2121(92)(29)(21) \qquad [D \to \pi\ell\nu, \text{Ref. [50]}], \tag{145}$$

$$N_f = 2+1\text{:}\ |V_{cs}| = 0.958(25)(5)(10) \qquad [D \to K\ell\nu, \text{Ref. [51]}], \tag{146}$$

where the uncertainties are lattice, experimental (plus nonlattice theory), and missing long-distance QED corrections (estimated to be 1%), respectively.

For $N_f = 2+1+1$, we update our BCL fit to the binned $D \to K\ell\nu$ differential decay rates by adding the FNAL/MILC 22 inputs for $f_+(q^2)$ and $f_0(q^2)$ at four q^2 values (the ETM 17D and HPQCD 21A inputs remain unchanged). The experimental datasets we include are unchanged with respect to FLAG 21 and are three different measurements of the $D^0 \to K^- e^+ \nu_e$ mode by BaBar (BaBar 07, Ref. [74]), CLEO-c (CLEO 09/0, Ref. [32]), and BESIII (BESIII 15, Ref. [75]); CLEO-c (CLEO 09/+, Ref. [32]) and BESIII measurements of the $D^+ \to \bar{K}^0 e^+ \nu_e$ mode (BESIII 17, Ref. [76]); and the recent first measurement of the $D^0 \to K^- \mu^+ \nu_\mu$ mode by BESIII, Ref. [77]. There is also a Belle dataset available in Ref. [78], but it provides results for parameterized form factors rather than partial widths, which implies that reverse modelling of the q^2-dependence of the form factor would be needed to add them to the fit, which involves an extra source of systematic uncertainty; it is, furthermore, the measurement with the largest error. Thus, we will drop it. The CLEO collaboration provides correlation matrices for the systematic uncertainties across the channels in their two measurements; the latter are, however, not available for BESIII, and, therefore, we will conservatively treat their systematics with a 100% correlation, following the same prescription as in the HFLAV review [73]. Since all lattice results have been obtained in the isospin limit, we average over the D^0 and D^+ electronic modes. The parameterization of the form factors we use here is the same as in the lattice-only fit discussed in Sec. 7.2, and we again increase the order of the z expansion (with respect to FLAG 21) to $N^+ = N^0 = 4$. In contrast to FLAG 21,

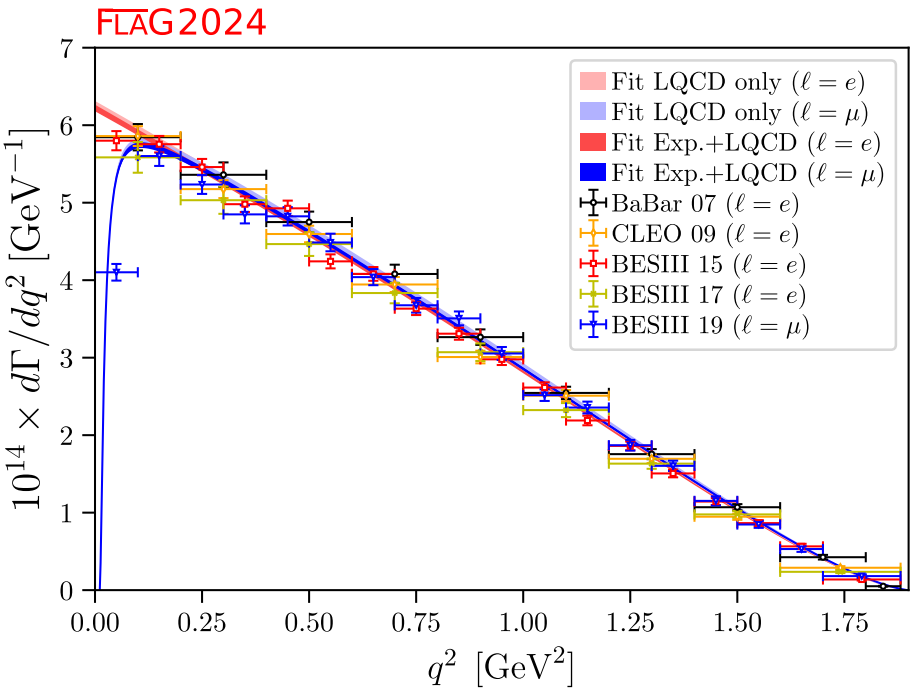

Figure 19: Our fits to the $D \to K\ell\nu$ differential decay rates used to determine $|V_{cs}|$, with experimental inputs from Refs. [32, 74–77] and lattice inputs from ETM17D [41], HPQCD 21A [43], and FNAL/MILC 22 [31].

we now include the short-distance electroweak correction $\eta_{\rm EW}^2$ [30] in the calculation of the differential decay rate, using $\eta_{\rm EW} = 1.009$ [31]. The fit has $\chi^2/\text{dof} \approx 1.66$ and we have scaled all uncertainties by a factor of $\sqrt{\chi^2/\text{dof}} \approx 1.29$. The results for the z-expansion parameters and $|V_{cs}|$, as well as their correlation matrix, are given in Tab. 32, and a plot of the differential decay rates is shown in Fig. 19. For $D \to \pi l\nu$, we do not use the lattice results away from $q^2 = 0$ as discussed in Sec. 7.2. To extract $|V_{cd}|$, we instead combine the average for $f_+^{D\pi}(0)$ from ETM 17D and FNAL/MILC 22 with the HFLAV result (144). Thus, we obtain

$$N_f = 2+1+1\text{: } |V_{cd}| = 0.2245(33)(22) \qquad [D \to \pi\ell\nu, \text{Ref. [31, 41]}], \tag{147}$$

$$N_f = 2+1+1\text{: } |V_{cs}| = 0.9592(50)(96) \qquad [D \to K\ell\nu, \text{Ref. [31, 41, 43]}], \tag{148}$$

where the two uncertainties correspond, respectively, to the combined lattice-QCD and experimental errors, and an estimate of the size of missing long-distance QED corrections, taken to be 1% following Ref. [31]. Note that FNAL/MILC 22 [31] also determined $|V_{cd}|$ from $D_s \to K\ell\nu$ using a BESIII measurement [79], with the result

$$N_f = 2+1+1\text{: } |V_{cd}| = 0.258(15)(03) \qquad [D_s \to K\ell\nu, \text{Ref. [31]}], \tag{149}$$

where the large uncertainty is dominated by the experimental measurement.

For $\Lambda_c \to \Lambda\ell\nu$, there are new experimental results for the electronic and muonic branching fractions from BESIII, published in 2022 and 2023 [80, 81]. In addition, the world average of the Λ_c lifetime has been updated in the 2024 Review of Particle Physics to $\tau_{\Lambda_c} = (202.6 \pm$

$D \to K\ell\nu$ ($N_f = 2+1+1$)

	values	correlation matrix							
a_0^+	0.7896(38)	1.	−0.555568	−0.069722	−0.021610	0.587914	0.646372	0.247552	0.795354
a_1^+	−0.945(51)	−0.555568	1.	−0.303470	0.102546	−0.014576	0.043616	0.036587	−0.280176
a_2^+	0.29(49)	−0.069722	−0.303470	1.	−0.109799	−0.092179	0.107676	0.243102	−0.033821
a_3^+	0.257(84)	−0.021610	0.102546	−0.109799	1.	−0.112476	0.104107	0.101692	−0.003737
a_0^0	0.7029(18)	0.587914	−0.014576	−0.092179	−0.112476	1.	0.341851	−0.256955	0.554412
a_1^0	0.748(32)	0.646372	0.043616	0.107676	0.104107	0.341851	1.	0.578012	0.651080
a_2^0	0.11(33)	0.247552	0.036587	0.243102	0.101692	−0.256955	0.578012	1.	0.279081
$\lvert V_{cs}\rvert$	0.9592(50)	0.795354	−0.280176	−0.033821	−0.003737	0.554412	0.651080	0.279081	1.

Table 32: Coefficients for the $N^+ = N^0 = 4$ z-expansion simultaneous fit of the $D \to K$ form factors f_+ and f_0 and $|V_{cs}|$ to the $D \to K\ell\nu$ differential decay rates and the ETM 17D, HPQCD 21A, and FNAL/MILC 22 lattice results. The form factors can be reconstructed using parameterization and inputs given in Appendix B.3.1.

1.0) $\times 10^{-15}$ s, following a new precise measurement by Belle II [82]. Using these results together with the lattice-QCD predictions of Meinel 16 for $\Gamma(\Lambda_c \to \Lambda\ell\nu)/|V_{cs}|^2$ [61], and including the factor of $\eta_{\rm EW}^2$ (not done in Ref. [61]), we obtain

$$N_f = 2+1\text{: } |V_{cs}| = 0.929(24)(16)(2)(9) \qquad [\Lambda_c \to \Lambda\ell\nu, \text{Ref. [61]}], \tag{150}$$

where the uncertainties are from the lattice calculation, from the $\Lambda_c \to \Lambda\ell\nu$ branching fractions, from the Λ_c lifetime, and from the missing long-distance QED corrections, respectively.

In Fig. 20, we summarize the results for $|V_{cd}|$ and $|V_{cs}|$ from leptonic and semileptonic decays, and compare them to determinations from neutrino scattering (for $|V_{cd}|$ only) and global fits assuming CKM unitarity (see [59, 83]). For both $|V_{cd}|$ and $|V_{cs}|$, the errors in the direct determinations from leptonic and semileptonic decays are approximately one order of magnitude larger than the indirect determination from CKM unitarity.

In order to provide final estimates, we average the available results from the different processes separately for each value of N_f and obtain

$$N_f = 2+1+1\text{: } \begin{cases} |V_{cd}| = 0.2229(64) \\ |V_{cs}| = 0.9667(96) \end{cases} \quad \text{[FLAG average, Refs. [6, 8, 31, 43]]}\,, \tag{151}$$

$$N_f = 2+1\text{: } \begin{cases} |V_{cd}| = 0.2165(49) \\ |V_{cs}| = 0.973(14) \end{cases} \quad \text{[FLAG average, Refs. [13, 16–19, 21, 50, 51, 61]]}\,, \tag{152}$$

where the errors include both theoretical and experimental uncertainties, and scale factors equal to $\sqrt{\chi^2/\text{dof}}$ of 1.88 and 1.26 have been included for $|V_{cd}|_{N_f=2+1+1}$ and $|V_{cs}|_{N_f=2+1}$, respectively. These averages also appear in Fig. 20, and are compatible with the values from the CKM global fit based on unitarity [83] within at most 1.5σ. The slight increases in the uncertainties of the $N_f = 2+1+1$ averages compared to FLAG 21 are due to the inclusion of QED systematic uncertainties (treated as 100% correlated between the different processes) and the scale factors. The large scale factor for $|V_{cd}|_{N_f=2+1+1}$ is caused by the $D_s \to K\ell\nu$ result that has large uncertainty but also a considerably higher central value. Removing this result would change the average to $|V_{cd}|_{N_f=2+1+1} = 0.2214(44)$.

Using the lattice determinations of $|V_{cd}|$ and $|V_{cs}|$ in Eqs. (151), (152) and $|V_{cb}| \approx 0.04$, we can test the unitarity of the second row of the CKM matrix. We obtain

$$N_f = 2+1+1\text{: } |V_{cd}|^2 + |V_{cs}|^2 + |V_{cb}|^2 - 1 = -0.01(2)$$
[FLAG average, Refs. [6, 8, 31, 43]], (153)

$$N_f = 2+1\text{: } |V_{cd}|^2 + |V_{cs}|^2 + |V_{cb}|^2 - 1 = 0.00(3)$$
[FLAG average, Refs. [13, 16–19, 21, 50, 51, 61]]. (154)

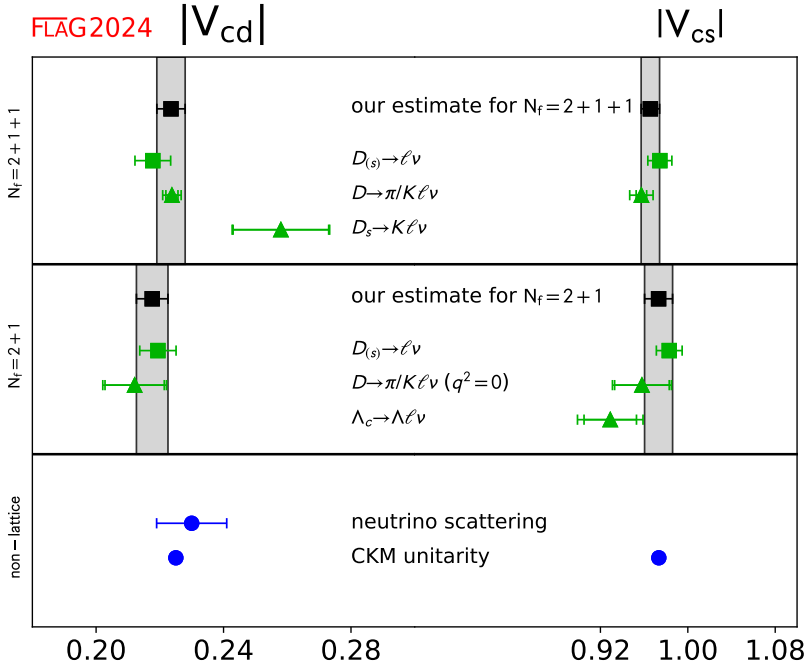

Figure 20: Comparison of determinations of $|V_{cd}|$ and $|V_{cs}|$ obtained from lattice methods [Eqs. (142), (143), (145), (146), (147), (148), (149), (150), (151), (152)] with a nonlattice determination from neutrino scattering (for $|V_{cd}|$ only) [59] and with the Standard-Model predictions from a global fit assuming CKM unitarity [83].

References

[1] [FLAG 21] Y. Aoki et al., *FLAG Review 2021*, *Eur. Phys. J. C* **82** (2022) 869 [2111.09849].

[2] [FLAG 19] S. Aoki et al., *FLAG Review 2019: Flavour Lattice Averaging Group (FLAG)*, *Eur. Phys. J. C* **80** (2020) 113 [1902.08191].

[3] Particle Data Group collaboration, *Review of particle physics*, *Phys. Rev. D* **110** (2024) 030001.

[4] [FLAG 13] S. Aoki, Y. Aoki, C. Bernard, T. Blum, G. Colangelo et al., *Review of lattice results concerning low-energy particle physics*, *Eur.Phys.J.* **C74** (2014) 2890 [1310.8555].

[5] [ETM 21B] P. Dimopoulos, R. Frezzotti, M. Garofalo and S. Simula, *K- and $D_{(s)}$-meson leptonic decay constants with physical light, strange and charm quarks by ETMC*, *PoS* **LATTICE2021** (2021) 472 [2110.01294].

[6] [FNAL/MILC 17] A. Bazavov et al., *B- and D-meson leptonic decay constants from four-flavor lattice QCD*, *Phys. Rev.* **D98** (2018) 074512 [1712.09262].

[7] [FNAL/MILC 14A] A. Bazavov et al., *Charmed and light pseudoscalar meson decay constants from four-flavor lattice QCD with physical light quarks*, *Phys.Rev.* **D90** (2014) 074509 [1407.3772].

[8] [ETM 14E] N. Carrasco, P. Dimopoulos, R. Frezzotti, P. Lami, V. Lubicz et al., *Leptonic decay constants f_K, f_D and f_{D_s} with $N_f = 2+1+1$ twisted-mass lattice QCD*, *Phys.Rev.* **D91** (2015) 054507 [1411.7908].

[9] [ETM 13F] P. Dimopoulos, R. Frezzotti, P. Lami, V. Lubicz, E. Picca et al., *Pseudoscalar decay constants f_K/f_π, f_D and f_{D_s} with $N_f = 2+1+1$ ETMC configurations*, *PoS* **LATTICE2013** (2014) 314 [1311.3080].

[10] [FNAL/MILC 13] A. Bazavov et al., *Charmed and strange pseudoscalar meson decay constants from HISQ simulations*, *PoS* **LATTICE2013** (2014) 405 [1312.0149].

[11] [FNAL/MILC 12B] A. Bazavov et al., *Pseudoscalar meson physics with four dynamical quarks*, *PoS* **LAT2012** (2012) 159 [1210.8431].

[12] [RQCD/ALPHA 24] S. Kuberski, F. Joswig, S. Collins, J. Heitger and W. Söldner, *D and $\mathrm{D_s}$ decay constants in $N_\mathrm{f} = 2+1$ QCD with Wilson fermions*, *JHEP* **07** (2024) 090 [2405.04506].

[13] [ALPHA 23] A. Bussone, A. Conigli, J. Frison, G. Herdoíza, C. Pena, D. Preti et al., *Hadronic physics from a Wilson fermion mixed-action approach: Charm quark mass and $D_{(s)}$ meson decay constants*, *Eur. Phys. J. C* **84** (2024) 506 [2309.14154].

[14] [χQCD 20A] Y. Chen, W.-F. Chiu, M. Gong, Z. Liu and Y. Ma, *Charmed and ϕ meson decay constants from 2+1-flavor lattice QCD*, *Chin. Phys. C* **45** (2021) 023109 [2008.05208].

[15] [RBC/UKQCD 18A] P. A. Boyle, L. Del Debbio, N. Garron, A. Juttner, A. Soni, J.T. Tsang et al., *SU(3)-breaking ratios for $D_{(s)}$ and $B_{(s)}$ mesons*, 1812.08791.

[16] [RBC/UKQCD 17] P. A. Boyle, L. Del Debbio, A. Jüttner, A. Khamseh, F. Sanfilippo and J.T. Tsang, *The decay constants $\mathbf{f_D}$ and $\mathbf{f_{D_s}}$ in the continuum limit of $\mathbf{N_f = 2+1}$ domain wall lattice QCD*, *JHEP* **12** (2017) 008 [1701.02644].

[17] [χQCD 14] Y. Yi-Bo et al., *Charm and strange quark masses and f_D_s from overlap fermions*, *Phys. Rev.* **D92** (2015) 034517 [1410.3343].

[18] [HPQCD 12A] H. Na, C.T. Davies, E. Follana, G.P. Lepage and J. Shigemitsu, *$|V_{cd}|$ from D meson leptonic decays*, *Phys.Rev.* **D86** (2012) 054510 [1206.4936].

[19] [FNAL/MILC 11] A. Bazavov et al., *B- and D-meson decay constants from three-flavor lattice QCD*, *Phys.Rev.* **D85** (2012) 114506 [1112.3051].

[20] [PACS-CS 11] Y. Namekawa et al., *Charm quark system at the physical point of 2+1 flavor lattice QCD*, *Phys.Rev.* **D84** (2011) 074505 [1104.4600].

[21] [HPQCD 10A] C. T. H. Davies, C. McNeile, E. Follana, G. Lepage, H. Na et al., *Update: precision D_s decay constant from full lattice QCD using very fine lattices*, *Phys.Rev.* **D82** (2010) 114504 [1008.4018].

[22] [HPQCD/UKQCD 07] E. Follana, C.T.H. Davies, G.P. Lepage and J. Shigemitsu, *High precision determination of the π, K, D and D_s decay constants from lattice QCD*, *Phys. Rev. Lett.* **100** (2008) 062002 [0706.1726].

[23] [FNAL/MILC 05] C. Aubin, C. Bernard, C.E. DeTar, M. Di Pierro, E.D. Freeland et al., *Charmed meson decay constants in three-flavor lattice QCD*, *Phys.Rev.Lett.* **95** (2005) 122002 [hep-lat/0506030].

[24] [RQCD 21] G. S. Bali, V. Braun, S. Collins, A. Schäfer and J. Simeth, *Masses and decay constants of the η and η' mesons from lattice QCD*, *JHEP* **08** (2021) 137 [2106.05398].

[25] D. Giusti, C.F. Kane, C. Lehner, S. Meinel and A. Soni, *Methods for high-precision determinations of radiative-leptonic decay form factors using lattice QCD*, *Phys. Rev. D* **107** (2023) 074507 [2302.01298].

[26] R. Frezzotti, N. Tantalo, G. Gagliardi, F. Sanfilippo, S. Simula, V. Lubicz et al., *Lattice calculation of the Ds meson radiative form factors over the full kinematical range*, *Phys. Rev. D* **108** (2023) 074505 [2306.05904].

[27] A. Desiderio et al., *First lattice calculation of radiative leptonic decay rates of pseudoscalar mesons*, *Phys. Rev. D* **103** (2021) 014502 [2006.05358].

[28] G. Parisi, *The Strategy for Computing the Hadronic Mass Spectrum*, *Phys. Rept.* **103** (1984) 203.

[29] G.P. Lepage, *The Analysis of Algorithms for Lattice Field Theory*, in *Theoretical Advanced Study Institute in Elementary Particle Physics*, 6, 1989.

[30] A. Sirlin, *Large m_W, m_Z behavior of the $O(\alpha)$ corrections to semileptonic processes mediated by W*, *Nucl.Phys.* **B196** (1982) 83.

[31] [FNAL/MILC 22] A. Bazavov et al., *D-meson semileptonic decays to pseudoscalars from four-flavor lattice QCD*, *Phys. Rev. D* **107** (2023) 094516 [2212.12648].

[32] CLEO collaboration, *Improved measurements of D meson semileptonic decays to π and K mesons*, *Phys. Rev.* **D80** (2009) 032005 [0906.2983].

[33] BESIII collaboration, *Measurement of $e^+e^- \to \pi^+\pi^-\psi(3686)$ from 4.008 to 4.600 GeV and observation of a charged structure in the $\pi^\pm\psi(3686)$ mass spectrum*, *Phys. Rev.* **D96** (2017) 032004 [1703.08787].

[34] BESIII collaboration, *Measurement of the branching fraction for the semi-leptonic decay $D^{0(+)} \to \pi^{-(0)}\mu^+\nu_\mu$ and test of lepton universality*, *Phys. Rev. Lett.* **121** (2018) 171803 [1802.05492].

[35] P.F. Bedaque, *Aharonov-Bohm effect and nucleon nucleon phase shifts on the lattice*, *Phys.Lett.* **B593** (2004) 82 [nucl-th/0402051].

[36] C. Sachrajda and G. Villadoro, *Twisted boundary conditions in lattice simulations*, *Phys.Lett.* **B609** (2005) 73 [hep-lat/0411033].

[37] [ETM 11B] S. Di Vita, B. Haas, V. Lubicz, F. Mescia, S. Simula and C. Tarantino, *Form factors of the $D \to \pi$ and $D \to K$ semileptonic decays with $N_f = 2$ twisted mass lattice QCD*, *PoS* **LATTICE2010** (2010) 301 [1104.0869].

[38] [HPQCD 11C] J. Koponen et al., *The D to K and D to π semileptonic decay form factors from lattice QCD*, *PoS* **LAT2011** (2011) 286 [1111.0225].

[39] [HPQCD 12B] J. Koponen, C. Davies and G. Donald, *D to K and D to π semileptonic form factors from lattice QCD, Charm 2012*, 1208.6242.

[40] [HPQCD 13C] J. Koponen, C.T.H. Davies, G.C. Donald, E. Follana, G.P. Lepage et al., *The shape of the $D \to K$ semileptonic form factor from full lattice QCD and V_{cs}*, 1305.1462.

[41] [ETM 17D] V. Lubicz, L. Riggio, G. Salerno, S. Simula and C. Tarantino, *Scalar and vector form factors of $D \to \pi(K)\ell\nu$ decays with $N_f = 2+1+1$ twisted fermions*, *Phys. Rev.* **D96** (2017) 054514 [1706.03017].

[42] [ETM 18] V. Lubicz, L. Riggio, G. Salerno, S. Simula and C. Tarantino, *Tensor form factor of $D \to \pi(K)\ell\nu$ and $D \to \pi(K)\ell\ell$ decays with $N_f = 2+1+1$ twisted-mass fermions*, *Phys. Rev.* **D98** (2018) 014516 [1803.04807].

[43] [HPQCD 21A] B. Chakraborty, W.G. Parrott, C. Bouchard, C.T.H. Davies, J. Koponen and G.P. Lepage, *Improved V_{cs} determination using precise lattice QCD form factors for $D \to K\ell\nu$*, *Phys. Rev. D* **104** (2021) 034505 [2104.09883].

[44] [FNAL/MILC 04] C. Aubin et al., *Semileptonic decays of D mesons in three-flavor lattice QCD*, *Phys.Rev.Lett.* **94** (2005) 011601 [hep-ph/0408306].

[45] V. Lubicz, G. Martinelli, M.S. McCarthy and C.T. Sachrajda, *Semileptonic decays of D mesons in a lattice QCD*, *Phys. Lett. B* **274** (1992) 415.

[46] A. Abada, D. Becirevic, P. Boucaud, J.P. Leroy, V. Lubicz and F. Mescia, *Heavy → light semileptonic decays of pseudoscalar mesons from lattice QCD*, *Nucl. Phys. B* **619** (2001) 565 [hep-lat/0011065].

[47] FOCUS collaboration, *Measurements of the q^2 dependence of the $D^0 \to K^-\mu^+\nu$ and $D^0 \to \pi^-\mu^+\nu$ form factors*, *Phys.Lett.* **B607** (2005) 233 [hep-ex/0410037].

[48] Belle collaboration, *Measurement of $D^0 \to \pi l\nu(Kl\nu)$ and their form-factors*, hep-ex/0510003.

[49] [FNAL/MILC 12G] J. A. Bailey et al., *Charm semileptonic decays and $|V_{cs(d)}|$ from heavy clover quarks and 2+1 flavor asqtad staggered ensembles*, *PoS* **LAT2012** (2012) 272 [1211.4964].

[50] [HPQCD 11] H. Na et al., *$D \to \pi\ell\nu$ semileptonic decays, $|V_{cd}|$ and 2^{nd} row unitarity from lattice QCD*, *Phys.Rev.* **D84** (2011) 114505 [1109.1501].

[51] [HPQCD 10B] H. Na, C.T.H. Davies, E. Follana, G.P. Lepage and J. Shigemitsu, *The $D \to K\ell\nu$ semileptonic decay scalar form factor and $|V_{cs}|$ from lattice QCD*, *Phys.Rev.* **D82** (2010) 114506 [1008.4562].

[52] [JLQCD 17B] T. Kaneko, B. Colquhoun, H. Fukaya and S. Hashimoto, *D meson semileptonic form factors in $N_f = 3$ QCD with Möbius domain-wall quarks*, *EPJ Web Conf.* **175** (2018) 13007 [1711.11235].

[53] G. Colangelo, M. Procura, L. Rothen, R. Stucki and J. Tarrus Castella, *On the factorization of chiral logarithms in the pion form factors*, *JHEP* **09** (2012) 081 [1208.0498].

[54] M. Marshall, P. Boyle, L. Del Debbio, F. Erben, J. Flynn, A. Jüttner et al., *Semileptonic $D \to \pi\ell\nu$, $D \to K\ell\nu$ and $D_s \to K\ell\nu$ decays with 2+1f domain wall fermions*, *PoS* **LATTICE2021** (2022) 416 [2201.02680].

[55] [ETM 10] R. Baron et al., *Light hadrons from lattice QCD with light (u,d), strange and charm dynamical quarks*, *JHEP* **1006** (2010) 111 [1004.5284].

[56] J. Bijnens and I. Jemos, *Hard Pion Chiral Perturbation Theory for $B \to \pi$ and $D \to \pi$ Formfactors*, *Nucl. Phys.* **B840** (2010) 54 [1006.1197], [Erratum: Nucl. Phys.B844,182(2011)].

[57] [HPQCD 22] W. G. Parrott, C. Bouchard and C.T.H. Davies, *$B \to K$ and $D \to K$ form factors from fully relativistic lattice QCD*, *Phys. Rev. D* **107** (2023) 014510 [2207.12468].

[58] [HPQCD 20] L. J. Cooper, C.T.H. Davies, J. Harrison, J. Komijani and M. Wingate, *$B_c \to B_{s(d)}$ form factors from lattice QCD*, *Phys. Rev. D* **102** (2020) 014513 [2003.00914], [Erratum: Phys.Rev.D 103, 099901 (2021)].

[59] Particle Data Group collaboration, *Review of Particle Physics*, *PTEP* **2020** (2020) 083C01.

[60] T. Feldmann and M.W.Y. Yip, *Form Factors for Lambda$_b \to \Lambda$ Transitions in SCET*, *Phys. Rev.* **D85** (2012) 014035 [1111.1844], [Erratum: Phys. Rev.D86,079901(2012)].

[61] S. Meinel, $\Lambda_c \to \Lambda l^+ \nu_l$ *form factors and decay rates from lattice QCD with physical quark masses*, *Phys. Rev. Lett.* **118** (2017) 082001 [1611.09696].

[62] BESIII collaboration, *Measurement of the absolute branching fraction for* $\Lambda_c^+ \to \Lambda e^+ \nu_e$, *Phys. Rev. Lett.* **115** (2015) 221805 [1510.02610].

[63] BESIII collaboration, *Measurement of the absolute branching fraction for* $\Lambda_c^+ \to \Lambda \mu^+ \nu_\mu$, *Phys. Lett.* **B767** (2017) 42 [1611.04382].

[64] S. Meinel, $\Lambda_c \to N$ *form factors from lattice QCD and phenomenology of* $\Lambda_c \to n\ell^+\nu_\ell$ *and* $\Lambda_c \to p\mu^+\mu^-$ *decays*, *Phys. Rev.* **D97** (2018) 034511 [1712.05783].

[65] W. Detmold, C. Lehner and S. Meinel, $\Lambda_b \to p\ell^-\bar{\nu}_\ell$ *and* $\Lambda_b \to \Lambda_c \ell^- \bar{\nu}_\ell$ *form factors from lattice QCD with relativistic heavy quarks*, *Phys. Rev.* **D92** (2015) 034503 [1503.01421].

[66] Q.-A. Zhang, J. Hua, F. Huang, R. Li, Y. Li, C.-D. Lu et al., $\Xi_c \to \Xi$ *Form Factors and* $\Xi_c \to \Xi \ell^+ \nu_\ell$ *Decay Rates From Lattice QCD*, *Chin. Phys. C* **46** (2022) 011002 [2103.07064].

[67] Belle collaboration, *Measurements of the branching fractions of semileptonic decays* $\Xi_c^0 \to \Xi^- \ell^+ \nu_\ell$ *and asymmetry parameter of* $\Xi_c^0 \to \Xi^- \pi^+$ *decay*, *Phys. Rev. Lett.* **127** (2021) 121803 [2103.06496].

[68] C. Farrell and S. Meinel, *Form factors for the charm-baryon semileptonic decay* $\Xi_c \to \Xi \ell \nu$ *from domain-wall lattice QCD*, *PoS* **LATTICE2023** (2024) 210 [2309.08107].

[69] S. Meinel and G. Rendon, $\Lambda_c \to \Lambda^*(1520)$ *form factors from lattice QCD and improved analysis of the* $\Lambda_b \to \Lambda^*(1520)$ *and* $\Lambda_b \to \Lambda_c^*(2595, 2625)$ *form factors*, *Phys. Rev. D* **105** (2022) 054511 [2107.13140].

[70] B.A. Dobrescu and A.S. Kronfeld, *Accumulating evidence for nonstandard leptonic decays of* D_s *mesons*, *Phys. Rev. Lett.* **100** (2008) 241802 [0803.0512].

[71] M. Di Carlo, D. Giusti, V. Lubicz, G. Martinelli, C. Sachrajda, F. Sanfilippo et al., *Light-meson leptonic decay rates in lattice QCD+QED*, *Phys. Rev. D* **100** (2019) 034514 [1904.08731].

[72] P. Boyle et al., *Isospin-breaking corrections to light-meson leptonic decays from lattice simulations at physical quark masses*, *JHEP* **02** (2023) 242 [2211.12865].

[73] [HFLAV 18] Y. Amhis et al., *Averages of b-hadron, c-hadron, and* τ*-lepton properties as of 2018*, *Eur. Phys. J. C* **81** (2021) 226 [1909.12524].

[74] BaBar collaboration, *Measurement of the hadronic form-factor in* $D^0 \to K^- e^+ \nu_e$ *1*, *Phys. Rev. D* **76** (2007) 052005 [0704.0020].

[75] BESIII collaboration, *Study of Dynamics of* $D^0 \to K^- e^+ \nu_e$ *and* $D^0 \to \pi^- e^+ \nu_e$ *Decays*, *Phys. Rev. D* **92** (2015) 072012 [1508.07560].

[76] BESIII collaboration, *Analysis of* $D^+ \to \bar{K}^0 e^+ \nu_e$ *and* $D^+ \to \pi^0 e^+ \nu_e$ *semileptonic decays*, *Phys. Rev. D* **96** (2017) 012002 [1703.09084].

[77] BESIII collaboration, *Study of the $D^0 \to K^-\mu^+\nu_\mu$ dynamics and test of lepton flavor universality with $D^0 \to K^-\ell^+\nu_\ell$ decays*, *Phys. Rev. Lett.* **122** (2019) 011804 [1810.03127].

[78] BELLE collaboration, *Measurement of D0 —> pi l nu (Kl nu) Form Factors and Absolute Branching Fractions*, *Phys. Rev. Lett.* **97** (2006) 061804 [hep-ex/0604049].

[79] BESIII collaboration, *First Measurement of the Form Factors in $D_s^+ \to K^0 e^+\nu_e$ and $D_s^+ \to K^{*0} e^+\nu_e$ Decays*, *Phys. Rev. Lett.* **122** (2019) 061801 [1811.02911].

[80] BESIII collaboration, *Study of the Semileptonic Decay $\Lambda_c^+ \to \Lambda e^+\nu e$*, *Phys. Rev. Lett.* **129** (2022) 231803 [2207.14149].

[81] BESIII collaboration, *Study of $\Lambda_c^+ \to \Lambda\mu^+\nu_\mu$ and test of lepton flavor universality with $\Lambda_c^+ \to \Lambda\ell^+\nu_\ell$ decays*, *Phys. Rev. D* **108** (2023) L031105 [2306.02624].

[82] BELLE-II collaboration, *Measurement of the Λ_c^+ Lifetime*, *Phys. Rev. Lett.* **130** (2023) 071802 [2206.15227].

[83] UTFIT collaboration, *New UTfit Analysis of the Unitarity Triangle in the Cabibbo-Kobayashi-Maskawa scheme*, *Rend. Lincei Sci. Fis. Nat.* **34** (2023) 37 [2212.03894].